Biomaterials 30 (2009) 556–564

Contents lists available at ScienceDirect

Biomaterials

journal homepage: www.elsevier.com/locate/biomaterials

The influence of fiber diameter of electrospun substrates on neural stem cell differentiation and proliferation

Gregory T. Christopherson [a], Hongjun Song [b], Hai-Quan Mao [a,c,*]

[a] Department of Materials Science and Engineering, Johns Hopkins University, 3400 N. Charles Street, Baltimore, MD 21218, USA
[b] Institute for Cell Engineering, Departments of Neurology and Neuroscience, Johns Hopkins University School of Medicine, 733 N. Broadway, Baltimore, MD 21205, USA
[c] Whitaker Biomedical Engineering Institute, Johns Hopkins University, 3400 N. Charles Street, Baltimore, MD 21218, USA

ARTICLE INFO

Article history:
Received 29 August 2008
Accepted 1 October 2008
Available online 31 October 2008

Keywords:
Neural stem cells
Differentiation
Proliferation
Nanotopography
Electrospun fiber
Fiber diameter

ABSTRACT

Neural stem/progenitor cells (NSCs) are capable of self-renewal and differentiation into all types of neural lineage under different biochemical and topographical cues. In this study, we cultured rat hippocampus-derived adult NSCs (rNSCs) on laminin-coated electrospun Polyethersulfone (PES) fiber meshes with average fiber diameters of 283 ± 45 nm, 749 ± 153 nm and 1452 ± 312 nm; and demonstrated that fiber diameter of PES mesh significantly influences rNSC differentiation and proliferation. Under the differentiation condition (in the presence of 1 μM retinoic acid and 1% fetal bovine serum), rNSCs showed a 40% increase in oligodendrocyte differentiation on 283-nm fibers and 20% increase in neuronal differentiation on 749-nm fibers, in comparison to tissue culture polystyrene surface. SEM imaging revealed that cells stretched multi-directionally to follow underlying 283-nm fibers, but extended along a single fiber axis on larger fibers. When cultured on fiber meshes in serum free medium in the presence of 20 ng/mL of FGF-2, rNSCs showed lower proliferation and more rounded morphology compared to that cultured on laminin-coated 2D surface. As the fiber diameter decreased, higher degree of proliferation and cell spreading and lower degree of cell aggregation were observed. This collective evidence indicates fiber topography can play a vital role in regulating differentiation and proliferation of rNSCs in culture.

1. Introduction

Neural stem/progenitor cells (NSCs) are intrinsically capable of differentiating into different neural cell types within the nervous system, offering prospects for NSC-based cell therapies to treat neurodegenerative diseases and traumatic injuries [1]. Major obstacles still impede the ability to apply neural stem cell therapies clinically, chief among which is the lack of efficient methodologies for large-scale expansion, as well as for controlled differentiation to functional cell types for transplantation. This is largely due to our limited understanding of mechanisms for NSC-fate specification and self-renewal. *In vivo*, NSCs are regulated by an array of physical, biochemical and topographical cues that constitute an essential part of their microenvironment [1]. Successful biochemical manipulation of rat adult NSCs has been achieved through supplementation of soluble growth factors to culture medium, for example, to promote NSC proliferation using FGF-2 [2] and to preferentially differentiate NSCs to neurons using retinoic acid and forskolin [3], to astrocytes using leukemia inhibitory factor (LIF) and bone morphogenic proteins (BMPs) [4], and to oligodendrocytes with insulin-like growth factor 1 (IGF-1) or platelet-derived growth factor (PDGF) [5,6]. Less understood is the impact of topographical cues on NSC proliferation and differentiation.

Basal lamina membrane in different tissues has unique nanofibrous characteristics [7], suggesting the importance of substrate topography. Additionally, a growing body of evidence demonstrates that micro-to-nanoscale topography plays an important role in controlling the adhesion, proliferation and survival of adult and embryonic stem cells in culture. For instance, human cord blood-derived hematopoietic stem progenitor cells exhibit increased proliferation and maintenance of progenitor markers when expanded on functionalized fibrous matrices [8], although the expansion efficiency is also influenced by surface functionalization scheme [9,10]. Micro and nanotopographies generated by colloidal lithography, electron beam lithography and polymer demixing techniques have been shown to promote the osteogenic differentiation of human bone marrow-derived osteoprogenitors [11,12]

* Corresponding author. Department of Materials Science and Engineering, School of Engineering, Johns Hopkins University, 102 Maryland Hall, 3400 N. Charles Street, Baltimore, MD 21218, USA. Tel.:+1 410 516 8792; fax: +1 410 516 5293.
E-mail address: hmao@jhu.edu (H.-Q. Mao).

0142-9612/$ – see front matter © 2008 Elsevier Ltd. All rights reserved.
doi:10.1016/j.biomaterials.2008.10.004

and human mesenchymal stem cells [13]. Similarly, osteoblast differentiation has been observed in MC3T3-E1 preosteoblast cells cultured on a nanofibrous poly(L-lactic acid) mesh prepared using phase separation method [10]. Rat hippocampal progenitor cells cultured on grooved substrates demonstrate increased cell alignment and neuronal differentiation [14]. Despite these studies, it remains unclear how topographical features (specifically, nanofiber diameter and alignment) influence stem cell proliferation and differentiation, partially due to the lack of a reliable method for producing fibers with well-defined diameters. We have recently developed a method that allows for electrospinning of fiber substrates with tightly controlled diameter distribution [15]. In this study we used this set of nanofibers to examine the effect of nanofiber diameter on rat adult neural stem/progenitor cell (rNSC) differentiation and proliferation, respectively, in comparison with two-dimensional substrates similarly modified by laminin-coating.

2. Materials and methods

2.1. Materials

Poly(ethersulfone) (PES) with M_w of 55,000 was purchased from Goodfellow Cambridge Limited, UK. Dimethyl Sulfoxide (DMSO) was purchased from JT Baker. Octadecyl Rhodamine B (R-18) and octadecyltrimethylammonium bromide (OTAB) were purchased from Sigma–Aldrich. Unless otherwise specified, all other reagents were purchased from Sigma–Aldrich.

2.2. Electrospinning of PES fibers

Electrospinning was conducted using a typical setup as we reported previously [8,9,15–17]. Using a high concentration of PES in DMSO (28% w/w) and low concentration of PES (20%), a stable Taylor cone forms [18], and nanofiber meshes were readily obtained with average diameters from over 2 μm down to 600 nm. Uniform nanofibers with diameter of less than 500 nm were difficult to obtain, as continued dilution of the PES solution resulted in loss of Taylor cone stability and then electrospraying. Supplementing PES solution with small molecular weight, amphiphilic dopant (R-18 or OTAB) further stabilized the polymer jet, yielding fibers as small as 250 nm with a narrow diameter distribution [15]. R-18 addition to PES resulted in fluorescent fibers, but with no discernable impact on cell viability. PES fiber scaffolds doped with OTAB were rinsed thoroughly with ethanol to remove the amphiphile. Experimental parameters used for spinning different sets of fibers are listed in Table 1. All fiber meshes were spun onto 15-mm glass coverslips layered on a grounded aluminum foil target, and then transferred to 24-well cell culture plates. Fiber meshes were secured to the coverslips by applying a small amount of surgical glue (B-401 secure adhesive, Factor II, Lakeside, AZ) to the edge of the coverslip. All fiber meshes were washed with water to remove residual DMSO, followed by a 60-min washing in 70% ethanol for sterilization prior to subsequent cell culture. To assess the average diameter, over 100 individual fibers were measured by NIH Image J software (NIH, Bethesda, MD) using SEM images from at least 5 different sections of each fiber sample.

2.3. Fiber surface coating with laminin and characterization

Laminin is a key component of the basement membrane, and the most efficient cell adhesion molecule for mediating rNSC adhesion when coated to a substrate surface [19]. Laminin-coating is typically achieved via a pre-adsorbed poly-L-ornithine (PLO) layer on the substrate surface [19]. All PES fiber meshes, PES films (spin-coated onto 15-mm glass coverslips), and tissue culture polystyrene (TCPS) plates were coated overnight with PLO (Sigma–Aldrich) solution in phosphate-buffered saline (PBS, 10 μg/mL) at room temperature and thoroughly rinsed with PBS. All substrates were then coated with laminin (Sigma–Aldrich) solution in PBS (5 μg/mL) for 14 h at 37 °C, and washed with PBS.

Table 1
Electrospinning parameters for preparation of fiber meshes with different diameters.

Solution composition (in DMSO)	Voltage (kV)	Collecting distance (cm)	Flow rate (mL/hr)	Needle size (Gauge)	Fiber diameter[a] (nm)
20% PES, 0.5% OTAB or R-18	12	20	0.3	27G	273 ± 45
22% PES	10	12	0.6	25G	749 ± 153
26% PES	12	12	1.0	22G	1452 ± 312

[a] Diameters are listed as mean ± standard deviation.

Surface density of coated laminin was characterized using ^{125}I-labeled laminin, which was prepared using IODO-GEN® Pre-Coated Iodination Tubes (Pierce, Rockford, IL) according to the Chizzonite indirect method as we previously described [20]. Briefly, 1.0 mCi of $Na^{125}I$ was mixed with 100 μL of Tris iodination buffer (TIB, 25 mM Tris-Cl, 0.4 M NaCl, pH 7.5) and activated at room temperature for 6 min in an IODO-GEN tube. Subsequently, the activated iodine was removed and added to 1 mL of laminin solution in PBS (1 mg/mL) and reacted for 8 min. The reaction mixture was then purified using a pre-equilibrated D-salt polyacrylamide desalting column (Pierce). A specific activity of approximately 1×10^8 cpm/mL was obtained for the laminin solution.

TCPS and PES fiber meshes ($n = 4$) were coated with PLO and ^{125}I-laminin as described above, washed with PBS three times, transferred to a glass test tube, and counted on a Packard Cobra Quantum gamma counter (Perkin Elmer Inc.). The mass of protein detected on the substrates was calculated from the radioactivity of the samples.

Fiber surface area was calculated using SEM images and Image J software. Area fractions were obtained by thresholding the SEM images ($n = 5$) and using the Image J measurement tool. Assumption of cylindrical fibers and disregarding fiber overlap allowed us to multiply the area fraction by π to obtain a rough estimation of fiber surface area for each sample type. The laminin surface density was calculated based on the surface area of the fiber meshes and the amount of adsorbed surface protein obtained from the radiolabeling.

2.4. Differentiation culture of rNSCs in the presence of fetal bovine serum and retinoic acid

The rNSCs were isolated and purified from Fischer 344 rat hippocampi, and propagated in laminin-coated flasks in DEME/F12 medium containing N2 supplement, L-glutamine (2 mM) and FGF-2 (20 ng/mL) as previously described [21]. These rNSCs were shown to give rise to neurons, oligodendrocytes and astrocytes both *in vitro* [19] and after transplantation *in vivo* [2] as previously shown. Cells used for this study were between passages 32 and 38. Differentiation of rNSCs was induced by supplementation of 1 μM of retinoic acid (RA) and 1% of fetal bovine serum (FBS) to the medium. Under this condition, rNSCs can be differentiated into a mixed lineage of neurons, astrocytes and oligodendrocytes [22]. Three typical sets of PES fiber meshes were used for this study with average diameters of 283 ± 45 nm, 749 ± 153 nm and 1452 ± 312 nm, respectively. These PES fiber meshes, PES films and TCPS wells ($n = 3$, for each staining condition) in 24-well plates were seeded with rNSCs at 10,000 cells/well in DMEM/F-12 cell culture medium with 1 ng/mL FGF-2 to maintain cell viability. After 24 h, RA and FBS were added to a final concentration of 1 μM and 1%, respectively. Cells were then cultured for 5 days before being processed for imaging and immunocytochemical analysis.

2.5. Proliferation culture of rNSCs in the presence of FGF-2

The same sets of substrates (PES fibers, PES films and TCPS) as described above were used for this investigation to characterize the effect of substrate topography on rNSC proliferation. Cell proliferative analysis was performed using 96-well plates that were created with various PES fibers. rNSCs were seeded at a concentration of 400 cells/well, and cultured in DMEM/F-12 medium containing N2 supplement, L-glutamine (2 mM), and various concentrations of FGF-2 (0, 0.5, 1, 5 and 20 ng/mL, $n = 10$ for each concentration). Cells were cultured for 5 days before analyzing the DNA content in each well using a CyQuant kit from Invitrogen (Carlsbad, CA) [20]. For immunofluorescence staining, cultures were performed in triplicates in 24-well plates with a cell-seeding density of 1000 cells/well in the proliferation medium with 20 ng/mL of FGF-2. A same set of culture was conducted without FGF-2 as controls. Cells were cultured for 5 days before being processed for imaging analysis.

2.6. Immunofluorescence staining and imaging of cultured rNSCs

Immunofluorescence staining was performed to characterize phenotypic changes to rNSCs that occurred over the course of proliferation or differentiation culture. Cells were washed with PBS, fixed in 4% paraformaldehyde at room temperature for 45 min, blocked and permeabilized using Tris-buffered saline (TBS) supplemented with 5% donkey serum and 0.25% Triton X-100 (TBS++) for 90 min. Primary antibodies were incubated for 90 min, and secondary antibodies were incubated for 60 min (each in TBS++), followed by DAPI staining [22]. Antibody panel used include primary antibody against nestin (neural progenitor marker, mouse, Chemicon, 1:1000 dilution), Tuj-1 (neuronal marker, rabbit, Covance, 1:1000), RIP (oligodendrocyte marker, mouse, Hybridoma, 1:500), GFAP (astrocyte marker, rabbit, DakoCytomation, 1:1000) and DAPI (nuclear staining), used for differentiation and proliferation conditions; Ki-67 (rabbit, Novocastra, 1:500) [23] was additionally used for proliferative investigation. Secondary antibodies include Cy-2 and Cy-3 conjugated anti-mouse and anti-rabbit antibodies (Jackson, 1:250). Immunofluorescence microscopy was performed using a Nikon TE2000 fluorescence microscope. Three samples of each substrate type were imaged, with overlapping staining combinations to minimize non-specific quantification. At least 20 images of each staining condition were captured at 200× magnification, thresholded (Adobe Photoshop CS) to remove any possible background, and manually counted to obtain positive stained fractions

(DAPI staining was used as counter staining). Over 1000 cells were counted for quantification of each marker.

2.7. Scanning electron microscope (SEM) analysis of the fibers and cells

Samples prepared for SEM analysis were fixed with a mixture of 1.5% glutaraldehyde/3% paraformaldehyde in 100 mM sodium cacodylate buffer (pH 7.4) with 2.5% sucrose for 45 min at room temperature before being post-fixed with 1% osmium tetroxide in 100 mM sodium cacodylate buffer for 15 min at room temperature. Samples were dehydrated with a graded ethanol series (50/75/85/95/100/100% in water) followed by hexamethyldisilizane (HMDS) or CO_2 critical-point drying (Samdri-795, Tousimis, Rockville, MD). Subsequent 10-nm platinum sputter-coating (Hummer 6.2 Sputter System, Anatech USA, Hayward, CA) allowed for imaging with environmental (FEI Quanta 200 ESEM, Hillsboro, OR) or field-emission SEM (JEOL 6700F, Tokyo, Japan).

3. Results

3.1. Preparation, modification and characterization of fiber substrates

PES fibers are amenable to surface functionalization through covalent grafting [15,17] or protein coating. Such versatility and its nondegradative nature make it an ideal substrate system for *ex vivo* culture. The PES–DMSO polymer-solvent combination is also a reliable and reproducible electrospinning system [15,17]. Fiber meshes with diameters ranging from 600–2000 nm can easily be prepared by electrospinning. By adopting our recently developed electrospinning method of doping the polymer solution with small molecular weight, amphiphilic molecules (R-18 or OTAB) [15], we prepared PES fibers with diameter as small as 250 nm with a tight diameter distribution. R-18 addition to PES resulted in R-18 entrapment, rendering fibers visible under fluorescence microscope, but with no discernable impact on cell viability [15]. We selected three sets of fiber meshes with diameters of 283 ± 45 nm (16%), 749 ± 153 nm (20%) and 1452 ± 312 nm (21%) to assess rNSC responses to these fiber substrates. Typical SEM micrographs of these three sets of fibers are shown in Fig. 1.

Rat NSCs are anchorage dependent cells; and LN has been shown to be an effective adhesion molecule supporting the adhesion and growth of rNSCs. We coated all fiber meshes with the well-adopted PLO–LN coating protocol [19]. Using ^{125}I-labeled LN, we characterized surface densities of LN on all different nanofibers in comparison with 2D tissue culture polystyrene (Fig. 1d). Our data confirmed that LN surface density obtained on PES fiber surface was independent of fiber diameter. LN surface density was about 123 ± 6 ng/cm^2, which is similar to that obtained on 2D TCPS surface.

3.2. Fiber diameter impacts rNSC differentiation in the presence of retinoic acid and serum

The effect of nanofiber diameter on rNSC differentiation was investigated in the presence of 1 μM retinoic acid (RA) and 1% fetal bovine serum (FBS), under which condition NSCs have been shown to differentiate into neurons, oligodendrocytes and astrocytes [19]. Cells were cultured for 5 days before immunofluorescence staining was performed to characterize the expression of Tuj-1 (neuronal marker), RIP (oligodendrocyte marker), GFAP (astrocyte marker), and nestin (neural stem/progenitor cell marker). As expected, a mix of Tuj-1$^+$ cells (38%), RIP$^+$ cells (8%) and GFAP$^+$ cells (17%) were observed on the TCPS surface (Fig. 2a). A large fraction (49%) of cells remained nestin positive, many of which co-expressed differentiated progenitor markers. There was predictably good cell spreading, indicating good cell migratory ability (Fig. 2b).

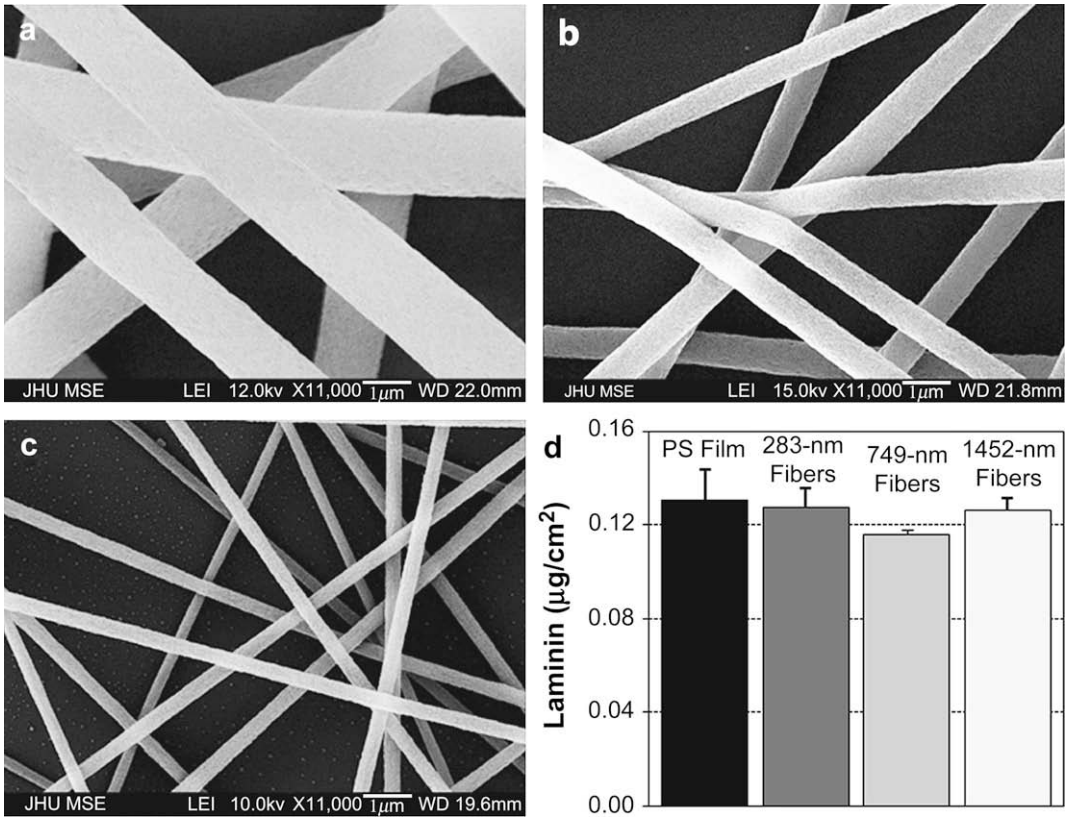

Fig. 1. SEM characterization of electrospun fiber meshes. (a) 283 ± 45 nm, prepared from 20% PES w/0.5% OTAB in DMSO; (b) 749 ± 153 nm, prepared from 22% PES in DMSO; and (c) 1452 ± 312 nm, prepared from 26% PES in DMSO. All images were obtained at 11,000× magnification; scale bars are 1 μm. The average surface densities of ^{125}I-labeled laminin on all fiber meshes and TCPS are shown in (d). Bars represent mean ± standard deviation ($n = 4$).

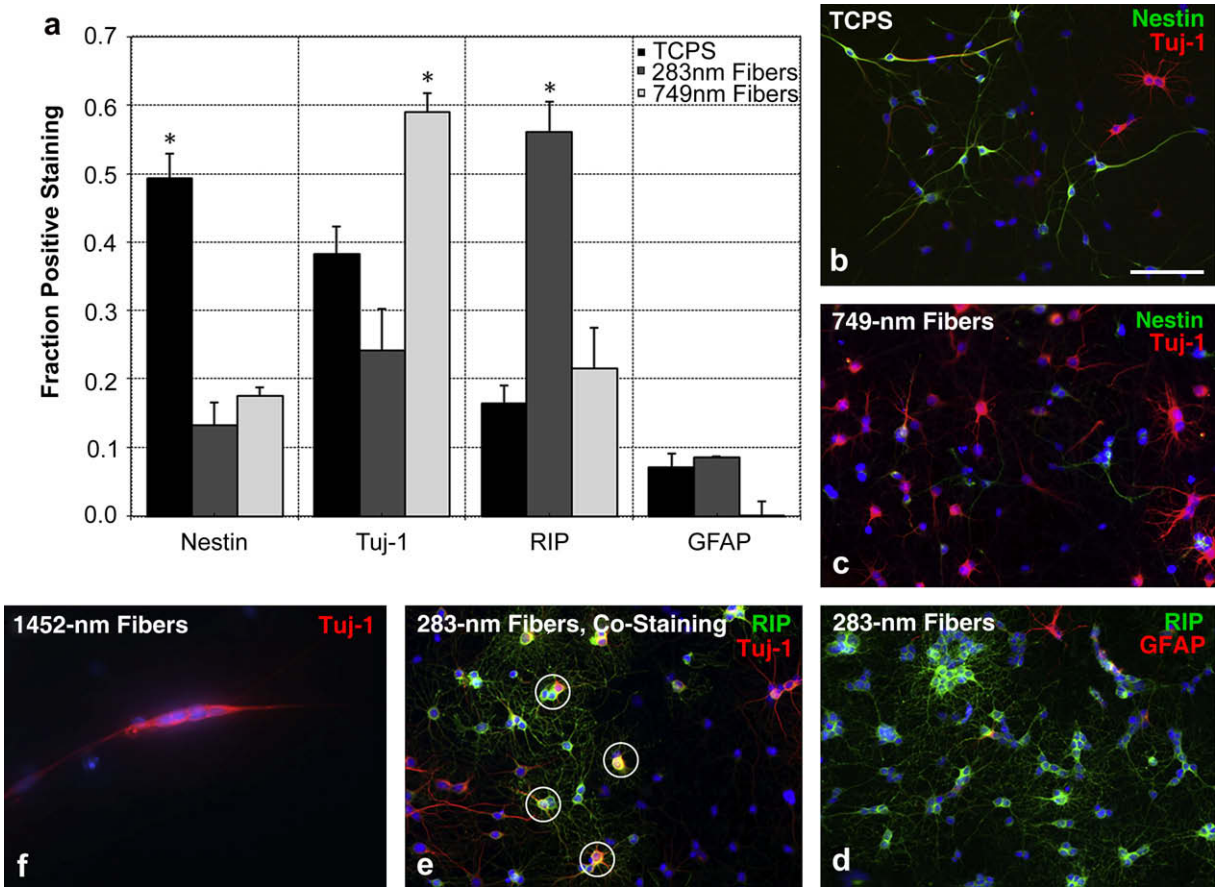

Fig. 2. Immunofluorescence analysis of rat NSCs cultured on various substrates in the presence of 1 μM retinoic acid and 1% fetal bovine serum for 5 days. Cell nuclei (blue) are stained using DAPI as a counter staining. Quantification of staining results is shown (a) with corresponding representative images of cells on each substrate (b–d). All images captured 200×, with scale bar = 100 μm. Error bars represent mean ± standard error ($n = 3$, more than 1000 cells were counted for each sample). Circled cells on 283-nm fiber mesh are cells stained double positive for RIP and Tuj-1 (e). Example of statistically unquantifiable 1452-nm mesh is shown in (f). *Denotes significant difference over all other samples ($p < 0.05$, unpaired 2-tail Student's t-test).

The differentiation of rNSCs cultured on electrospun fiber substrates was significantly different from that on the TCPS surface. On nanofibers with an average diameter of 283 nm (hereafter termed "283-nm fibers"), there was a 3-fold increase in the percentage of RIP$^+$ cells when compared to the TCPS control, and a 40% drop in the percentage of nestin$^+$ cells. There was no difference in the fraction of astrocytic differentiation (GFAP$^+$ cells) compared to TCPS control, and slightly lower Tuj-1 expression on 283-nm fibers ($p = 0.10$, Student's t-test). The immunofluorescence staining images shown in Fig. 2d revealed a striking contrast compared with cells cultured on other substrates. The dense dendrite extension staining, characteristic of oligodendrocytes, was apparent for 56% of the cells on 283-nm fibers. In contrast, rNSCs cultured on fibers with an average diameter of 749 nm ("749-nm fibers") yielded the highest fraction of neuronal differentiation among all substrates tested. There was negligible number of GFAP$^+$ cells found on 749-nm fibers, with a similar decrease in nestin+ cell fraction as to 283-nm fibers, indicating similar levels of differentiation of rNSCs on both fiber substrates. Tuj-1 staining image (Fig. 2c) revealed cell morphology consistent with that of neuronal precursors. Rat NSCs cultured on fibers with an average diameter of 1452 nm ("1452-nm fibers") showed lower viability by day 5. It was difficult to count sufficient number of cells (typically ≤ 5 per view under 200× field) for statistical analysis. Nevertheless, the majority of viable cells visible on 1452-nm fibers aligned along single fibers and expressed Tuj-1 (Fig. 2f).

In addition, cells cultured on fiber substrates showed higher levels of expression of the differentiation markers than those on TCPS surface. More interestingly, a significantly higher fraction of cells (7–10%) stained highly positive for both Tuj-1 and RIP (Fig. 2e). These are likely bi-potential "neuro-oligodendroglial" progenitors. Such bi-potential progenitors, representing an intermediate stage in NSC differentiation, have also been reported previously among cells differentiated from rat and human NSCs [20,24]. The exact identity and potential of these cells remain to be characterized.

3.3. Morphological changes of differentiating rNSCs cultured on fibers with different diameters

A fraction of samples that underwent differentiation as described above were processed for SEM imaging in order to visualize cell-substrate interaction. The morphological changes observed under SEM further confirmed the phenotypic analysis results. Different types of neural cells showed unique morphology as observed on TCPS surface with no apparent dominant cell type; oligodendrocytes exhibited a stretched and radiant network of dendrites (Fig. 3a), astrocytes appeared star-like (Fig. 3b) and neurons elongated along a preferred axis (Fig. 3a, and c). In stark contrast, the majority of cells observed on 283-nm fibers took on a fully stretched morphology, similar to that of oligodendrocytes, likely a result of contact guidance by the nanofiber matrix (Fig. 3d–f). Cells with neuronal and astrocytic morphologies were also present but at much lower fractions. Differentiation of rNSCs on 749-nm fibers yielded more cells showing morphology similar to that of neuronal progenitors. Cells were able to adhere and spread on

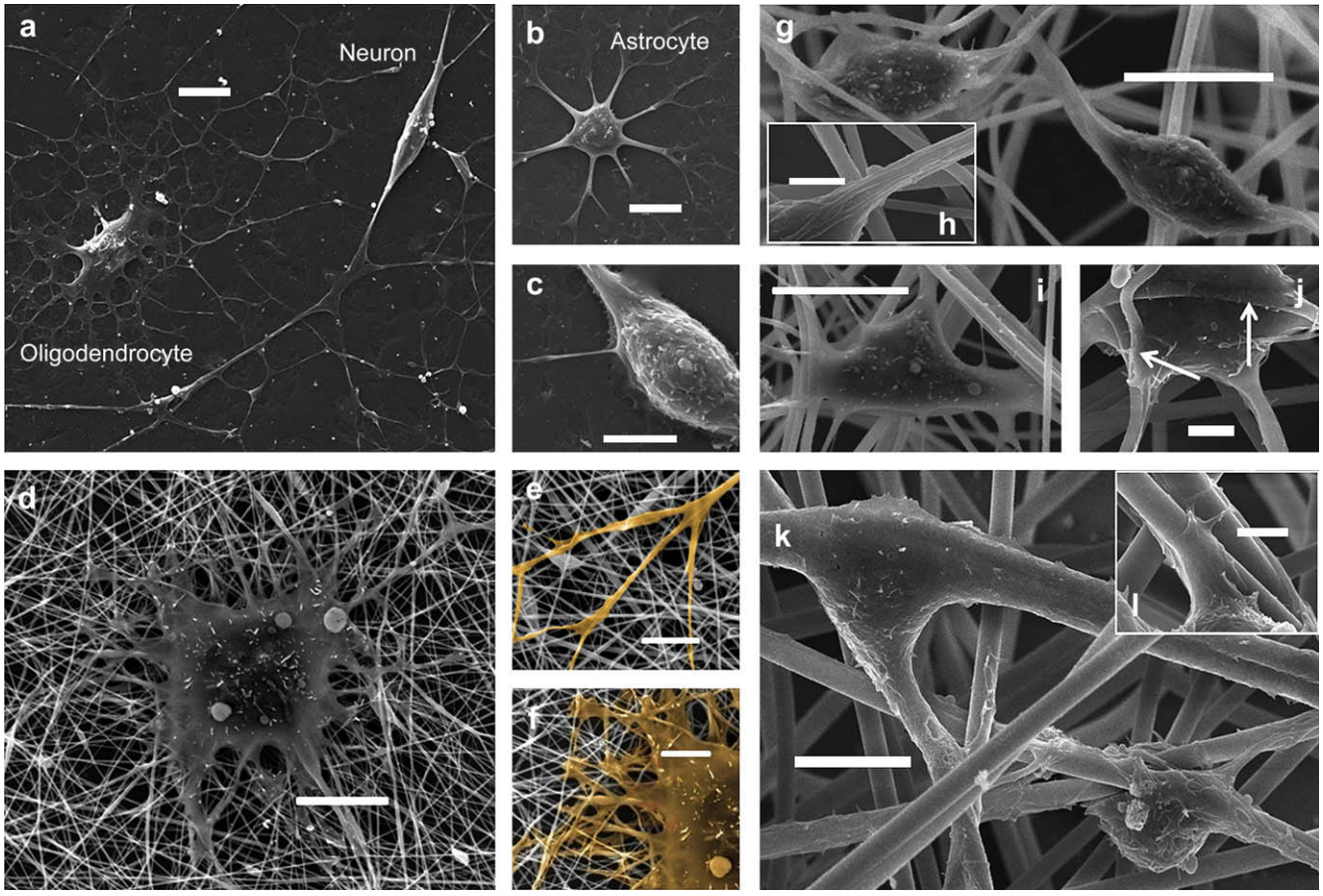

Fig. 3. SEM images of rat NSCs cultured on various substrates in the presence of 1 μM retinoic acid and 1% fetal bovine serum for 5 days. (a–c) Cells cultured on laminin-coated PES films; (d–f) Cells on 283-nm fiber mesh (cells are highlighted in yellow in (e) and (f)); (g–j) Cells on 749-nm fibers (cell attachment to fibers are indicated by arrows in (i) and (j)); (k, l) Cells on 1452-nm fibers. Scale bars for (a, b, d, g, i, k) are 10 μm, for (c, e, f) are 5 μm, and for (h, j, l) are 2 μm.

multiple fibers (Fig. 3i and j), but extending along a preferred fiber axis (Fig. 3g and h). A smaller fraction of cells stretched across multiple points where several fibers converge (Fig. 3i and j). Much lower fraction of cells was observed on 1452-nm fibers after 5-days of culture, likely due to the difficulty for rNSCs to adhere and migrate on larger fibers. Survived cells adhered on one or two fibers and elongated along the fiber axis (Fig. 3k and l) showing a morphology indicative of neurons or neuronal progenitors.

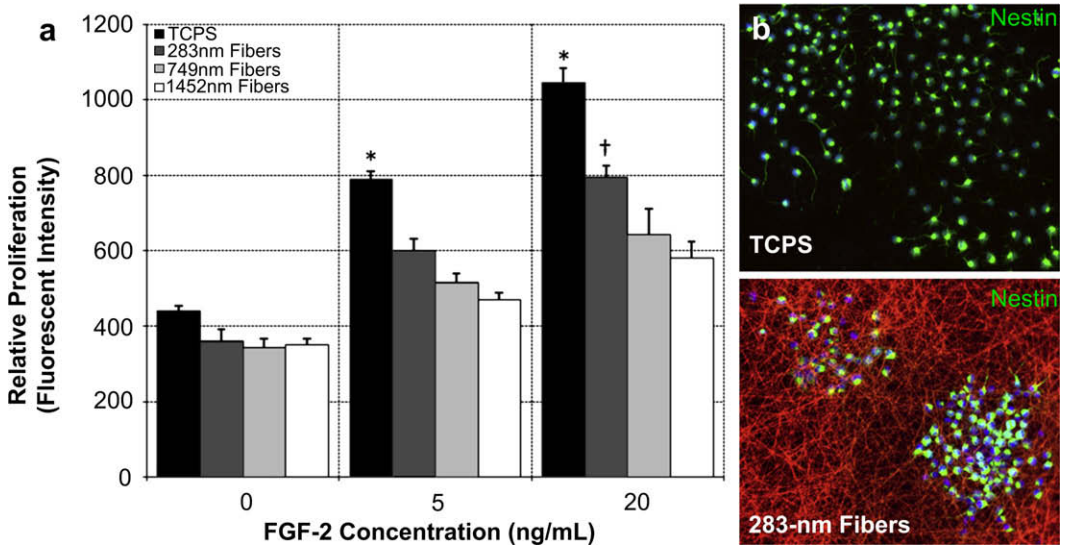

Fig. 4. Quantification and immunofluorescence imaging of rat NSCs cultured in serum free medium and 20 ng/mL of FGF-2 for 5 days. (a) Effect of fiber diameter on cell proliferation rate. Bars represent mean ± standard deviation ($n = 10$); (b) Immunofluorescence images of cells cultured on laminin-coated TCPS and 283-nm fibers, which were doped with R-18 to reveal underlying fiber substrate. Cell nuclei (blue) are stained using DAPI as a counter staining. * and † denote statistical significance ($p < 0.05$) over all other groups, and other fiber substrates, respectively.

3.4. Effect of fiber diameter on rNSC proliferation in the presence of FGF-2

In order to characterize the effect of fiber diameter on rNSC proliferation, we expanded rNSCs in serum free medium in the presence of 0, 5 and 20 ng/mL of FGF-2, a sufficient mitogen for rNSC proliferation [19,21]. Rat NSC proliferation was characterized by relative increase of total DNA content in cell lysate after 5 days of culture. Among all substrates tested, TCPS surface was the most effective to promote rNSC proliferation, resulting in the highest cell

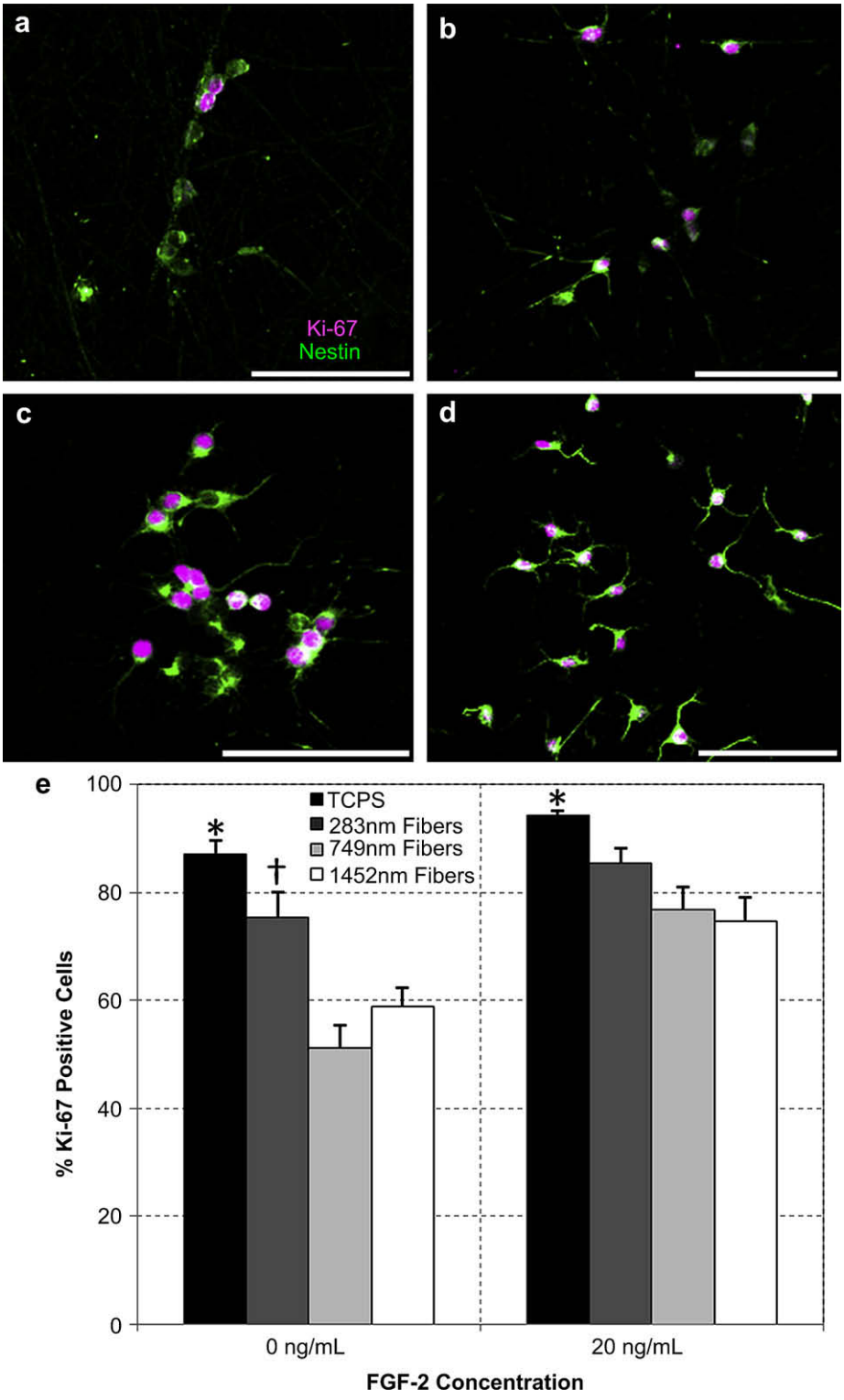

Fig. 5. Effect of fiber diameter on fraction of proliferating cells in serum free medium in the absence or presence of 20 ng/mL of FGF-2 for 5 days. Shown are representative images of Ki-67 antibody-stained cells cultured on 1452-nm fibers (a), 749-nm fibers (b), 283-nm fibers (c), and TCPS (d) in the absence of FGF-2. Scale bars are 100 μm. Quantitative analysis of fraction of Ki-67 positive cells is shown in (e). Bars represent mean ± standard deviation ($n \geq 10$); * and † denote statistical significance ($p < 0.05$) over all other groups, and other fiber substrates, respectively.

number under various FGF-2 concentrations. As the fiber diameter increased, cell proliferation rate generally decreased (Fig. 4a). As expected, an increase in FGF-2 concentration generally increased rNSC proliferation on all fiber and TCPS substrates, but FGF-2 appeared to enhance fiber diameter impact on rNSC proliferation rate. In the absence of FGF-2, no significant difference was observed among fibers of different diameters. When the medium was supplemented with 20 ng/mL of FGF-2, the biggest difference was detected between 283-nm fibers and fibers with larger diameters. In addition to a decreased proliferation rate, the rNSCs cultured on fiber meshes exhibited drastically different collective characteristics, forming tight and distinct individual colonies. This is in contrast to the typical rNSC spreading seen on laminin-coated TCPS surfaces (Fig. 4b). This is examined in greater detail below by SEM.

To further confirm the DNA quantification results, we characterized the effect of fiber diameter on percentage of proliferative cells, identified by positive Ki-67 staining [23] (Fig. 5a–d). The percentage of Ki-67$^+$ cells cultured on different substrates in the presence (20 ng/mL) and absence of FGF-2 are shown in Fig. 5e. Phenotypic analysis (immunofluorescence staining for nestin, RIP, GFAP and Tuj-1 expression) was also conducted to verify the proliferation of rNSCs. Staining for differentiated cell types (RIP$^+$ oligodendrocytes, GFAP$^+$ astrocytes, and Tuj-1$^+$ neurons) was negligible on all substrates, and nearly 100% cells stained nestin positive. Similar to the proliferation assay results, the highest percentage of rNSCs remaining in the proliferation state was found for the TCPS surface among all substrates tested both in the absence and presence of 20 ng/mL of FGF-2, and the percentage of Ki-67$^+$ cells decreased as fiber diameter increased. Interestingly, the effect of fiber diameter on the fraction of proliferative cells was more pronounced in the absence of FGF-2 – increasing fiber diameter from 283 nm to 749 nm significantly reduced the fraction of Ki-67$^+$ cells from 76% to 50%. In contrast, the corresponding difference in the presence of 20 ng/mL of FGF-2 became statistically insignificant ($0.05 < p < 0.10$).

3.5. Morphological changes of proliferating rNSCs on different substrates

Rat NSCs cultured on TCPS or PES 2D substrates were well-spread across the entire surface as observed under fluorescence microscopy. Conversely, cells grown on 283-nm fibers were clustered – though well adhered – with slight spreading; individual colonies were distinct from one another. Such a trend was more pronounced for rNSCs cultured on fibers with larger diameters. These observations are more apparent by examining SEM images (Fig. 6) obtained from cells cultured on different substrates with 20 ng/mL of FGF-2. rNSCs cultured on PES films spread more uniformly across the substrate. In contrast, cells cultured on fiber substrates were clustered and assumed more rounded morphology. On 283-nm fibers, rNSCs in the clusters remained single cells but cell-cell adhesion was apparent. Cells cultured on 749-nm fibers

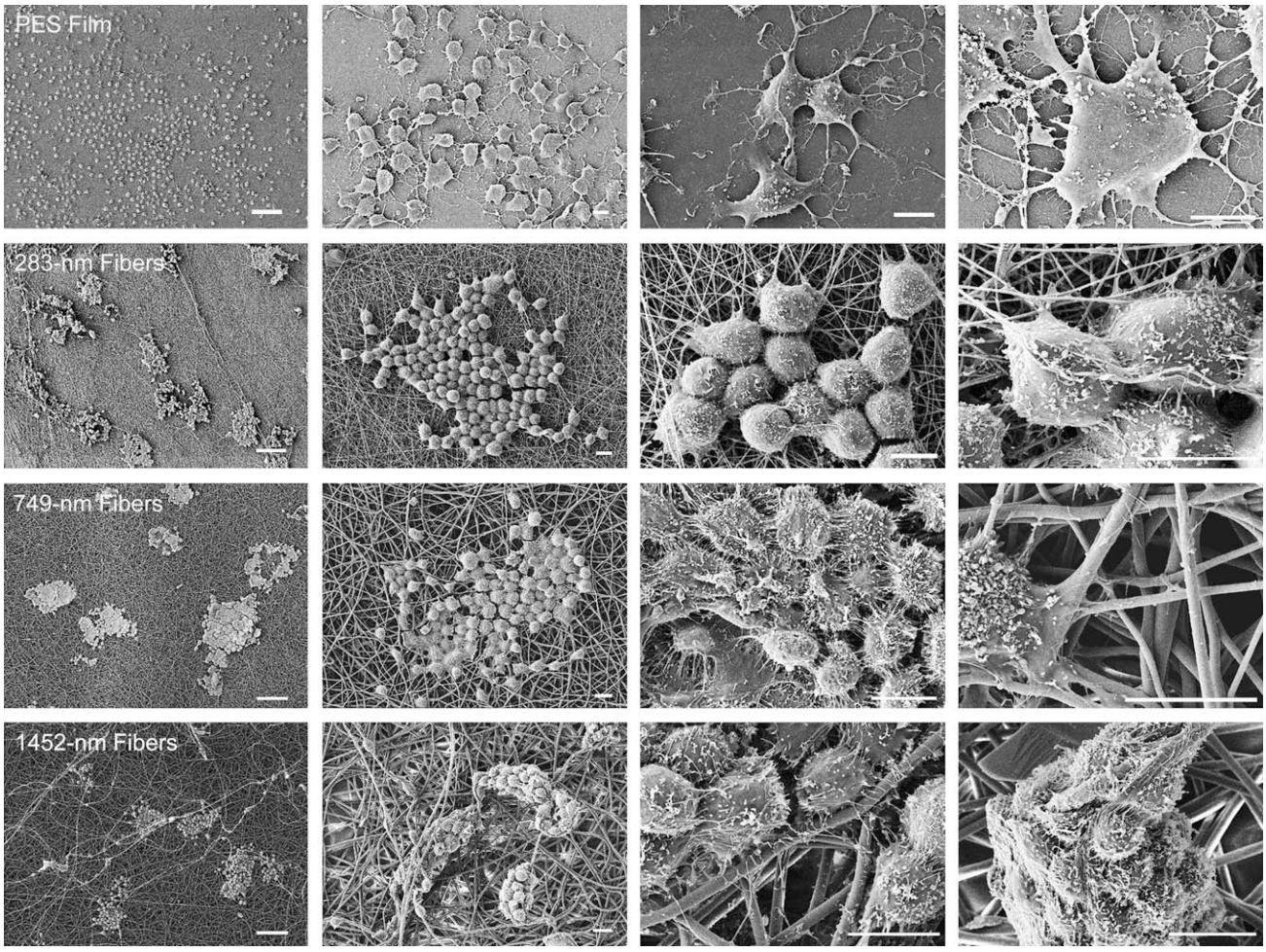

Fig. 6. SEM images of rat NSCs cultured in serum free medium and 20 ng/mL FGF-2 for 5 days. Scale bars for low magnification images (first column) are 100 μm; all other scale bars are 10 μm.

developed more cell-cell interaction, while maintaining substantial cell-fiber adhesion. Fewer colonies were observed on 1452-nm fibers and cells developed 3D-like multi-cell clusters resembling neurospheres [25], although a small fraction of cells remained adhered to fibers.

4. Discussion

Accumulative evidence suggests that nanofiber matrixes can partially mimic the topographical features of the natural extracellular matrix, influencing cell behavior synergistically with long-range and short-range biochemical cues. Systematic characterization of nanotopographical regulation of cell behavior is important to understanding and eventually engineering an artificial niche for *ex vivo* manipulation of stem cells. In this study, we used a series of electrospun fibrous substrates to quantitatively characterize the effect of fiber diameter of the substrates on rat adult NSC proliferation and differentiation. Compared to those reported in the literature, fiber matrixes used in this study have much narrower diameter distribution [26–29]. Moreover, all fiber surfaces were coated with similar density of laminin. These characteristics allow us to attribute cell behavior directly to fiber diameter.

Our results demonstrate that the diameter of fibers significantly influence cell adhesion and the ability of cells to migrate on the substrates. This leads to different consequences for rNSCs cultured under proliferation versus differentiation condition. Under proliferation condition (serum free medium with 20 ng/mL of FGF-2), rNSCs were able to adhere, spread and migrate extensively on a 2D surface, whereas rNSCs cultured on 283-nm fibers spread moderately and maintained more rounded morphology. Rat NSCs cultured on fibers with larger diameters showed lower migratory activity and developed large aggregates. Faster proliferation rate and a higher percentage of proliferative rNSCs cultured on a 2D substrate, together with a decreasing trend of cell proliferation on fiber substrates as fiber diameter increases (Figs. 4 and 5), suggested that cell spreading and actin fiber formation might be factors that enhance cell proliferation.

Differentiated rNSCs spread more extensively, spanning tens to a hundred microns across. Adhesion and migratory activity may play more important roles on their differentiation kinetics and lineage specification. Lower adhesion and limited migratory ability of rNSCs on larger fibers (749-nm and 1452-nm) have significantly reduced the survival of these cells in comparison with 283-nm fibers and a 2D surface. Interestingly, due to the higher migratory activity of these differentiating cells, fiber substrates guided the extension of cell processes and perhaps determined the morphology of the differentiating cells: cells on 283-nm fibers were able to spread along the nanofiber matrix randomly and assumed cell morphology of glial lineage; cells on larger fibers were able to extend on single fibers due to the size restriction, assuming cell shape similar to that of differentiated neurons. This fiber substrate-guided cell shape development correlates well with cell phenotypes obtained on different substrates. Despite the fact that a selective force is at play here for the larger diameter fibers – cells that differentiated into glial lineages could not spread well and assume their corresponding shapes or could not survive well. The strong correlation between fiber diameter, cell shape/morphology and phenotype suggests the possibility of shape regulation of rNSC lineage specification. These results warrant more studies to unravel mechanisms of substrate topographical control over stem cell proliferation and differentiation.

5. Conclusions

A well-defined fiber substrate platform was developed with controlled fiber diameter and variability, and a defined surface density of the cell adhesion ligand laminin. Using this platform, we have demonstrated that fiber diameter is an important parameter that impacts the adhesion, spreading, migration, proliferation and lineage specification of rNSCs under expansion and differentiation conditions. As the fiber diameter increases, rNSCs show reduced migration, spreading and proliferation in the presence of FGF-2 and serum free medium. Under the differentiation condition (in 1 μM retinoic acid and 1% FBS), rNSCs spread and assume glial cell shape and preferentially differentiate into oligodendrocytes, whereas they elongate on 749-nm and 1452-nm fibers and preferentially differentiate into neuronal lineage. These results suggest that topographical cues, when applied in conjunction with targeted biochemical signals, may be an instructive tool to regulate the lineage specification of stem cells.

Acknowledgements

This study was supported by National Science Foundation Faculty Early Career Award (DMR-0748340) and Maryland Stem Cell Research Commission (2007-MSCRFE-018). G.T.C. was supported by National Defense Science and Engineering Graduate (NDSEG) Fellowship and is a graduate scholar of Achievement Rewards for College Scientists (ARCS) Foundation. The authors thank Shawn Lim (Department of Biomedical Engineering, Johns Hopkins University), Dr. Stephen Fischer (Department of Materials Science and Engineering, JHU) and Xingyu Liu (DMSE, JHU) for technical help and discussion. Technical assistance from Mark Koontz (DMSE) and Michael McCaffery (Integrated Imaging Center, JHU) for SEM imaging is acknowledged. The authors also thank Dr. Yuan Chuan Lee for the assistance and support for ^{125}I-labeling experiments.

References

[1] Ming GL, Song HJ. Adult neurogenesis in the mammalian central nervous system. Annual Review of Neuroscience 2005;28:223–50.
[2] Gage FH, Coates PW, Palmer TD, Kuhn HG, Fisher LJ, Suhonen JO, et al. Survival and differentiation of adult neuronal progenitor cells transplanted to the adult brain. Proceedings of the National Academy of Sciences of the United States of America 1995;92(25):11879–83.
[3] Zhang XD, Cai J, Klueber KM, Guo ZF, Lu CL, Winstead WI, et al. Role of transcription factors in motoneuron differentiation of adult human olfactory neuroepithelial-derived progenitors. Stem Cells 2006;24(2):434–42.
[4] Nakashima K, Yanagisawa M, Arakawa H, Kimura N, Hisatsune T, Kawabata M, et al. Synergistic signaling in fetal brain by STAT3-Smad1 complex bridged by p300. Science 1999;284(5413):479–82.
[5] Hsieh J, Aimone JB, Kaspar BK, Kuwabara T, Nakashima K, Gage FH. IGF-1 instructs multipotent adult neural progenitor cells to become oligodendrocytes. Journal of Cell Biology 2004;164(1):111–22.
[6] Hu JG, Fu SL, Wang YX, Li Y, Jiang XY, Wang XF, et al. Platelet-derived growth factor-AA mediates oligodendrocyte lineage differentiation through activation of extracellular signal-regulated kinase signaling pathway. Neuroscience 2008;151(1):138–47.
[7] Birk DE, Trelstad RL. Extracellular compartments in matrix morphogenesis – Collagen fibril, bundle, and lamellar formation by corneal fibroblasts. Journal of Cell Biology 1984;99(6):2024–33.
[8] Chua KN, Chai C, Lee PC, Tang YN, Ramakrishna S, Leong KW, et al. Surface-aminated electrospun nanofibers enhance adhesion and expansion of human umbilical cord blood hematopoietic stem/progenitor cells. Biomaterials 2006;27(36):6043–51.
[9] Chua KN, Tang YN, Quek CH, Ramakrishna S, Leong KW, Mao HQ. A dual-functional fibrous scaffold enhances P450 activity of cultured primary rat hepatocytes. Acta Biomaterialia 2007;3(5):643–50.
[10] Hu J, Liu X, Ma PX. Induction of osteoblast differentiation phenotype on poly(l-lactic acid) nanofibrous matrix. Biomaterials 2008;29(28):3815–21.
[11] Dalby MJ, McCloy D, Robertson M, Agheli H, Sutherland D, Affrossman S, et al. Osteoprogenitor response to semi-ordered and random nanotopographies. Biomaterials 2006;27(15):2980–7.
[12] Hart A, Gadegaard N, Wilkinson CDW, Oreffo ROC, Dalby MJ. Osteoprogenitor response to low-adhesion nanotopographies originally fabricated by electron beam lithography. Journal of Materials Science-Materials in Medicine 2007;18(6):1211–8.

[13] Dalby MJ, Gadegaard N, Tare R, Andar A, Riehle MO, Herzyk P, et al. The control of human mesenchymal cell differentiation using nanoscale symmetry and disorder. Nature Materials 2007;6(12):997–1003.
[14] Recknor JB, Sakaguchi DS, Mallapragada SK. Directed growth and selective differentiation of neural progenitor cells on micropatterned polymer substrates. Biomaterials 2006;27(22):4098–108.
[15] Lin K, Chua KN, Christopherson GT, Lim S, Mao HQ. Reducing electrospun nanofiber diameter and variability using cationic amphiphiles. Polymer 2007;48(21):6384–94.
[16] Chua KN, Lim WS, Zhang P, Lu H, Wen J, Ramakrishna S, et al. Stable immobilization of rat hepatocyte spheroids on galactosylated nanofiber scaffold. Biomaterials 2005;26(15):2537–47.
[17] Chua KN, Chai C, Lee PC, Ramakrishna S, Leong KW, Mao HQ. Functional nanofiber scaffolds with different spacers modulate adhesion and expansion of cryopreserved umbilical cord blood hematopoietic stem/progenitor cells. Experimental Hematology 2007;35(5):771–81.
[18] Li D, Xia YN. Electrospinning of nanofibers: reinventing the wheel? Advanced Materials 2004;16(14):1151–70.
[19] Song H, Stevens CF, Gage FH. Astroglia induce neurogenesis from adult neural stem cells. Nature 2002;417(6884):39–44.
[20] Fischer SE, Liu XY, Mao HQ, Harden JL. Controlling cell adhesion to surfaces via associating bioactive triblock proteins. Biomaterials 2007;28(22):3325–37.
[21] Palmer TD, Takahashi J, Gage FH. The adult rat hippocampus contains primordial neural stem cells. Molecular and Cellular Neuroscience 1997;8(6):389–404.
[22] Takahashi J, Palmer TD, Gage FH. Retinoic acid and neurotrophins collaborate to regulate neurogenesis in adult-derived neural stem cell cultures. Journal of Neurobiology 1999;38(1):65–81.
[23] Ge SY, Goh ELK, Sailor KA, Kitabatake Y, Ming GL, Song HJ. GABA regulates synaptic integration of newly generated neurons in the adult brain. Nature 2006;439(7076):589–93.
[24] Orion Biosolutions. Novel neuro-glial progenitors express both b-tubulin III and GFAP. Webpage 2008. Available from: http://www.stemcellresources.org/library_images.html [accessed 15.08.08].
[25] Dottori M, Leung J, Turnley AM, Pebay A. Lysophosphatidic acid inhibits neuronal differentiation of neural stem/progenitor cells derived from human embryonic stem cells. Stem Cells 2008;26(5):1146–54.
[26] Badami AS, Kreke MR, Thompson MS, Riffle JS, Goldstein AS. Effect of fiber diameter on spreading, proliferation, and differentiation of osteoblastic cells on electrospun poly(lactic acid) substrates. Biomaterials 2006;27(4):596–606.
[27] Moroni L, Licht R, de Boer J, de Wijn JR, van Blitterswijk CA. Fiber diameter and texture of electrospun PEOT/PBT scaffolds influence human mesenchymal stem cell proliferation and morphology, and the release of incorporated compounds. Biomaterials 2006;27(28):4911–22.
[28] Shin M, Yoshimoto H, Vacanti JP. In vivo bone tissue engineering using mesenchymal stem cells on a novel electrospun nanofibrous scaffold. Tissue Engineering 2004;10(1-2):33–41.
[29] Yang F, Murugan R, Wang S, Ramakrishna S. Electrospinning of nano/micro scale poly(L-lactic acid) aligned fibers and their potential in neural tissue engineering. Biomaterials 2005;26(15):2603–10.